

Structure effects on fission yields

Bharat Kumar^{a,b}, M.T. Senthil kannan^c, M. Balasubramaniam^c, B. K. Agrawal^{b,d}, S. K. Patra^{a,b*}

^a*Institute of Physics, Sachivalaya Marg, Bhubaneswar - 751005, India.*

^b*Homi Bhabha National Institute, Anushakti Nagar, Mumbai - 400094, India.*

^c*Department of Physics, Bharathiar University, Coimbatore - 641046, India.*

^d*Saha Institute of Nuclear Physics, 1/AF, Bidhannagar, Kolkata - 700064, India.*

Abstract

The structure effects of the fission fragments on their yields are studied within the statical theory with the inputs, like, excitation energies and level density parameters for the fission fragments at a given temperature calculated using the temperature dependent relativistic mean field formalism (TRMF). For the comparison, the results are also obtained using the finite range droplet model. At temperatures $T = 1 - 2$ MeV, the structural effects of the fission fragments influence their yields. It is also seen that at $T = 3$ MeV, the fragments become spherical and the fragments distribution peaks at a close shell or near close shell nucleus.

Keywords: Nuclear fission, Level density, Heavy particle decay, Binding energies and masses

PACS: 25.85.-w, 23.70.+j, 21.10.Ma, 21.10.Dr

1. Introduction

Nuclear fission is still not completely understood, although it was discovered eight decades ago. The study of fission mass distribution is one of the major insight of the fission process. Conventionally, there are two different approaches, the statistical and the dynamical approaches for the study of fission process [1, 2]. The latter is a collective calculations of the potential energy surface and the mass asymmetry. Further, the fission fragments were determined either as the minima in the potential energy surface or by the maximum in the WKB penetration probability integral for the fission fragments. The statistical theory [2], begins with the statistical equilibrium is established from the saddle to scission point and the relative probability of the fission process depends on the density of the quantum states of the fragments at scission point. The mass and the charge distribution of the binary and the ternary fission is studied using the single particle energies of the finite range droplet model (FRDM) [3, 4, 5]. In FRDM [6] formalism, the energies at given temperature are calculated using the relation $E(T) = \sum_i n_i \epsilon_i$ with n_i and ϵ_i are the fermi-distribution function and the single-particle energy corresponding to the ground state deformation [4]. The temperature dependence of the deformations of the fission fragments and the contributions of the pairing correlations are also ignored. In the present letter, we applied the self consistent temperature dependent relativistic mean field theory (TRMF) with the well known NL3 parameter set [7, 8]. Here, we study the structure effects of the fission fragments, whether they could influence the yield or not? If it

influences, to what extent of the temperature it affects the probable fragmentation.

The letter is organized as follows. In Section 2, we present a brief description of the statistical theory and the TRMF formalism. In Section 3, we discuss the variation of the quadrupole deformation parameter β_2 of the fragments with the temperature and study the structure effects of the fission fragments in the mass distribution. The summary and conclusions of our results are given in Section 4.

2. The method

We constraint the charge to mass ratio of the fission fragments to that of the parent nucleus i.e., $Z_P/A_P \approx Z_i/A_i$, with A_P , Z_P and A_i , Z_i ($i = 1$ and 2) correspond to mass and charge number of the parent nucleus and fission fragments, respectively [3]. The constraints, $A_1 + A_2 = A$ and $Z_1 + Z_2 = Z$ are imposed to account for the mass and charge conservations. For ^{242}Pu , which is a representative case in the present study, the binary charge numbers are restricted to $Z_2 \geq 26$ and $Z_1 \leq 66$ by considering the experimental yield [9]. According to statistical theory [2, 10], the probability of the particular fragmentation is directly proportional to the folded level density ρ_{12} of that fragments with the total excitation energy E^* .

$$\rho_{12}(E^*) = \int_0^{E^*} \rho_1(E_1^*) \rho_2(E^* - E_1^*) dE_1^*. \quad (1)$$

The folded level density is calculated from the fragment level densities ρ_i [3, 5] with the excitation energy E_i^* and the level

*Corresponding author

Email address: patra@iopb.res.in (S. K. Patra^{a,b})

density parameters a_i ($i = 1$ and 2), which is given as:

$$\rho_i(E_i^*) = \frac{1}{12} \left(\frac{\pi^2}{a_i} \right)^{1/4} E_i^{*(-5/4)} \exp\left(2\sqrt{a_i E_i^*}\right). \quad (2)$$

Here, we used the self consistent temperature dependent relativistic mean field theory [7, 8] to calculate the excitation energy of the fragments. The excitation energies are calculated using the total energy for a given temperature and the ground state energy ($T = 0$) as, $E_i^* = E(T) - E(T = 0)$. Further, we calculate the excitation energies of the fragments using the ground state single particle energies of Finite Range Droplet Model (FRDM) [6] at the given temperature T with the help of the Fermi-Dirac distribution function keeping the total particle number conserved. The level density parameters a_i are evaluated from the excitation energies and the temperature as $a_i = E_i^*/T^2$. The relative yield is estimated as the ratio between the probability of a given fragmentation and the sum of the probabilities of all the possible fragmentations and it is given by,

$$Y(A_j, Z_j) = \frac{P(A_j, Z_j)}{\sum P(A_j, Z_j)}. \quad (3)$$

Here, the sum of the total probability is normalized to the scale 2. The competing basic decay modes such as neutron emission and α decay are not considered and the presented results are the prompt disintegration of a parent nucleus into two fragments (democratic breakup).

The well known relativistic mean field theory considers the nucleon nucleon interaction via effective mesons. The nucleon-meson interaction Lagrangian density are found in [11, 12, 8]. The TRMF formalism is explained in Refs. [7, 8]. Here, we briefly revisit the RMF with the BCS formalism. For open shell nuclei the pairing is important for the shell structure. The constant pairing gap BCS approximation is used in our calculations. The pairing interaction energy in terms of occupation probabilities v_i^2 and $u_i^2 = 1 - v_i^2$ is written as [13, 14]:

$$E_{pair} = -G \left[\sum_{i>0} u_i v_i \right]^2, \quad (4)$$

with G is the pairing force constant. The variational approach with respect to the occupation number v_i^2 gives the BCS equation $2\epsilon_i u_i v_i - \Delta(u_i^2 - v_i^2) = 0$ with the pairing gap $\Delta = G \sum_{i>0} u_i v_i$. The pairing gap (Δ) of proton and neutron is taken from the empirical formula [11], $\Delta = 12 \times A^{-1/2}$ MeV. The temperature is introduced in the partial occupancies in the BCS approximation as:

$$n_i = v_i^2 = \frac{1}{2} \left[1 - \frac{\epsilon_i - \lambda}{\tilde{\epsilon}_i} [1 - 2f(\tilde{\epsilon}_i, T)] \right], \quad (5)$$

with the function $f(\tilde{\epsilon}_i, T) = 1/(1 + \exp[\tilde{\epsilon}_i/T])$ represents the Fermi Dirac distribution; $\tilde{\epsilon}_i = \sqrt{(\epsilon_i - \lambda)^2 + \Delta^2}$ is the quasi particle energies and the ϵ_i is the single particle energies. In lower temperatures, the pairing energies play an important role in the structure of open shell nuclei. The chemical potential $\lambda_p(\lambda_n)$ for protons (neutrons) is obtained from the particle number constraints $\sum_i n_i^Z(n_i^N) = Z(N)$. The sum is taken over all proton and

neutron states. The entropy is obtained by,

$$S = - \sum_i [n_i \ln n_i + (1 - n_i) \ln(1 - n_i)]. \quad (6)$$

The temperature dependent RMF binding energies and the gap parameter are obtained by minimizing the free energy,

$$F = E - TS. \quad (7)$$

In constant pairing gap calculation, for a particular value of pairing gap Δ and force constant G , the pairing energy E_{pair} diverges, if it is extended to an infinite configuration space. Therefore, a pairing window in all the equations are extended up-to the level $|\epsilon_i - \lambda| \leq 2(41A^{-1/3})$ as a function of the single particle energy [11, 14].

3. Results and discussions

In this letter we study the fission fragment distributions of ^{242}Pu as a representative case. After generating the possible fragments by equating the charge to mass ratio of the parents to the charge-mass ratio of the fragments, the yield values are obtained using Eq. 3. The folded densities are calculated from the individual level density of the fragments which are evaluated from the fragment excitation energies at the given temperature T . The excitation energies are calculated within the TRMF and FRDM. In TRMF model, the excitation energy is the difference between the temperature dependent total energy and the ground state energy. The minimization of free energy of fission fragments within TRMF are obtained by allowing them to be axially deformed. The solutions for the Dirac equations for nucleons and the Klein Gordon equations for the meson fields are obtained by expanding them in terms of the spherical harmonic wave functions as basis. For the numerical calculations, the nucleon wave functions and the meson fields are expanded to the number of major shells taken to be $N_F = 12$ and $N_B = 20$, respectively. In the FRDM method, the excitation energies are calculated using the single particle energies which are retrieved

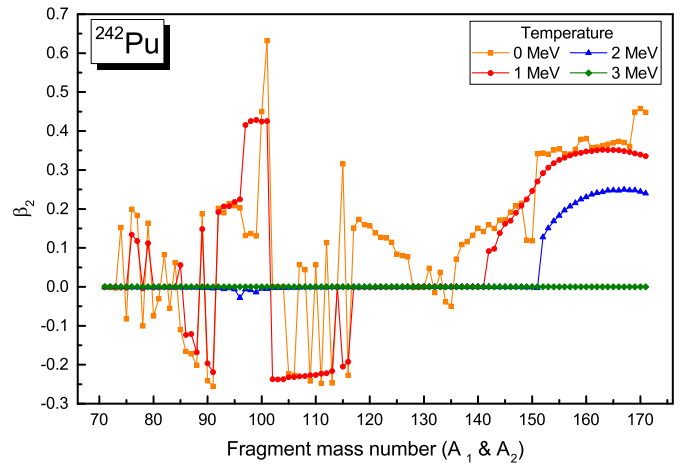


Figure 1: (color online) The variation of the quadrupole deformation parameter β_2 for the fission fragments for ^{242}Pu at temperature $T = 0-3$ MeV.

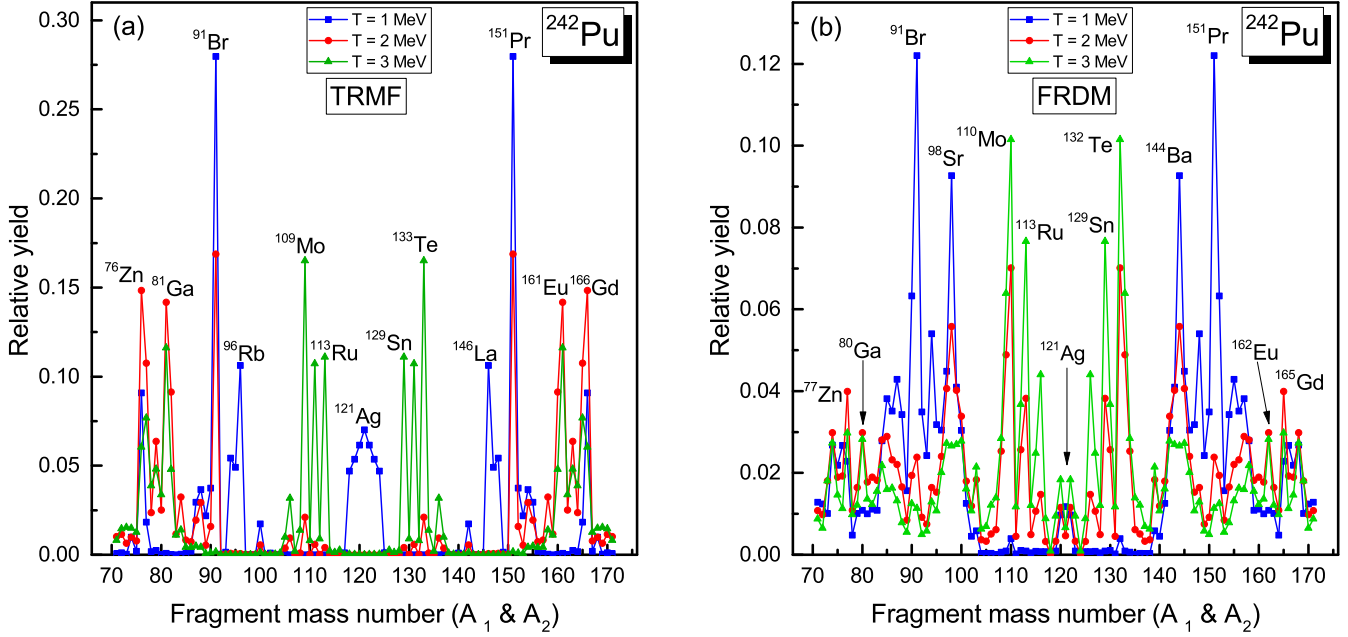


Figure 2: (color online) Mass distribution of ^{242}Pu for the three different temperatures $T = 1, 2$ and 3 MeV using the TRMF and FRDM formalisms. The sum of the total yield is normalized to the scale 2.

from the Reference Input Parameter Library (RIPL-3) [15] and the details of calculations can be found in Refs. [4, 5].

In Fig. 1 we plot the quadrupole deformation parameter β_2 as a function of mass numbers A_1 and A_2 for the binary fragments. For $T = 1$ MeV, the quadrupole deformation parameter of the fragments are prolate/oblate or spherical similar to the ground state nuclei. The pairing transition of the nuclei occur within the temperature $T = 1$ MeV. For $T = 2$ MeV, the fragments with mass number $A \leq 150$ become almost spherical except few exceptions. For higher temperature $T = 3$ MeV, all the nuclei become perfectly spherical. When the temperature increases, the levels above the Fermi surface become more occupied due to the transition of particles from the partial occupied levels (below the Fermi surface). For higher temperatures, the occupancies become uniform at the vicinity of the Fermi surface. The deformed structures are melted at higher temperatures, and the evolved fragments land up in a close shell shape due to the higher excitation energy of the closed shell nuclei.

Now the fission mass distributions of ^{242}Pu obtained from the TRMF and FRDM formalisms for three different temperatures $T = 1, 2$ and 3 MeV are shown in Fig. 2 and the fragment yields are compared in table 1. For $T = 1$ MeV, the most favorable fragmentation is $^{91}\text{Br} + ^{151}\text{Pr}$, for both the models. However, other fragments such as $^{96}\text{Rb} + ^{146}\text{La}$ in TRMF and $^{98}\text{Sr} + ^{144}\text{Ba}$ in FRDM are also noticed. In addition, the binary fragmentations $^{121,122}\text{Ag} + ^{121,120}\text{Ag}$ are favorable for both models. At temperature $T = 2$ and 3 MeV the yields of the minor fragments evolution in FRDM model have increased. But, in TRMF model, the most favorable fragments are mainly from the two regions, I (with mass $A \sim 71 - 91$ and $A \sim 171 - 151$) and II ($A \sim 105 - 113$ and $137 - 129$). For $T = 2$ MeV, region II is less probable than region I. The most favorable fragments

are same as those for temperature $T = 1$ MeV, along with one of the neutron closed shell nucleus in $^{81}\text{Ga} + ^{161}\text{Eu}$ (for ^{81}Ga , $N=50$). Analyzing Fig. 2(a) for TRMF results, we notice a symmetric yield region for $T = 3$ MeV, i.e. from mass region $A \sim 100 - 133$. Most of the yield fragments are concentrated in this region. Additionally, a few more secondary asymmetric fractions are also noticed. We see a similar symmetric region along with few asymmetric yields in case of FRDM calculations also (see Fig. 2(b)). The only difference is the secondary asymmetric yields spread widely in this case, contrary to the concentrated symmetric peaks for TRMF calculations. In general, our results agree with the recent experimental observations of Ref. [16].

In FRDM model, the favorable fragments are in the vicinity of the neutron closed shell ($N = 82$) nuclei or exactly at the proton closed shell nuclei ($Z = 50$). The other secondary fragmentations are not necessarily closed shell nuclei, so a good fraction of non-magic fragments are also appeared in the yield values. For higher temperature $T = 3$ MeV, the most favorable fragments for both models are more or less same. The fragment combinations $^{109,110}\text{Mo} + ^{133,132}\text{Te}$ and $^{113}\text{Ru} + ^{129}\text{Sn}$ are the most favorable fragments. In TRMF model the most favorable fragments in region I and region II have sharp peak yield values. But in FRDM, the larger yields are at region II only. Conclusively, for $T = 3$ MeV, one of the most favorable fragments are at the vicinity of the closed shell ($N \sim 82$) or exactly at the closed shell (N or $Z = 50$) nuclei. As it is reported in many earlier works, that the rare earth nuclei in the range $Z = 56 - 66$ region shows, peculiar nature, such as shell closure behavior, most of the fragments are found in that region. Also, the corresponding neutron numbers for such nuclei act like deformed shell closure at $N = 98 - 102$ region. As a result,

Table 1: The relative fission yield (R.Y.)= $Y(A_j, Z_j) = \frac{P(A_j, Z_j)}{\sum P(A_j, Z_j)}$ obtained at temperature $T = 1, 2$ and 3 MeV from the TRMF calculations are compared with the FRDM prediction for ^{242}Pu . The sum of the total yield is normalized to the scale 2.

T (MeV)	TRMF		FRDM	
	Fragment	R.Y.	Fragment	R.Y.
1	$^{91}\text{Br} + ^{151}\text{Pr}$	0.559	$^{91}\text{Br} + ^{151}\text{Pr}$	0.244
	$^{96}\text{Rb} + ^{146}\text{La}$	0.213	$^{98}\text{Sr} + ^{144}\text{Ba}$	0.184
	$^{76}\text{Zn} + ^{166}\text{Gd}$	0.182	$^{90}\text{Br} + ^{152}\text{Pr}$	0.120
	$^{121}\text{Ag} + ^{121}\text{Ag}$	0.140	$^{94}\text{Rb} + ^{148}\text{La}$	0.108
	$^{120}\text{Ag} + ^{122}\text{Ag}$	0.122	$^{97}\text{Sr} + ^{145}\text{Ba}$	0.088
	$^{94}\text{Rb} + ^{148}\text{La}$	0.108	$^{87}\text{Se} + ^{155}\text{Nd}$	0.086
	$^{119}\text{Pd} + ^{123}\text{Cd}$	0.107	$^{99}\text{Sr} + ^{143}\text{Ba}$	0.082
	$^{95}\text{Rb} + ^{147}\text{La}$	0.098	$^{85}\text{As} + ^{157}\text{Pm}$	0.076
2	$^{91}\text{Br} + ^{151}\text{Pr}$	0.336	$^{110}\text{Mo} + ^{132}\text{Te}$	0.140
	$^{76}\text{Zn} + ^{166}\text{Gd}$	0.295	$^{98}\text{Sr} + ^{144}\text{Ba}$	0.110
	$^{81}\text{Ga} + ^{161}\text{Eu}$	0.282	$^{97}\text{Sr} + ^{145}\text{Ba}$	0.080
	$^{77}\text{Zn} + ^{165}\text{Gd}$	0.213	$^{99}\text{Sr} + ^{143}\text{Ba}$	0.079
	$^{82}\text{Ge} + ^{160}\text{Sm}$	0.182	$^{113}\text{Ru} + ^{129}\text{Sn}$	0.076
	$^{79}\text{Ga} + ^{163}\text{Eu}$	0.125	$^{100}\text{Y} + ^{142}\text{Cs}$	0.068
	$^{109}\text{Mo} + ^{133}\text{Te}$	0.329	$^{110}\text{Mo} + ^{132}\text{Te}$	0.202
3	$^{81}\text{Ga} + ^{161}\text{Eu}$	0.295	$^{113}\text{Ru} + ^{129}\text{Sn}$	0.152
	$^{113}\text{Ru} + ^{129}\text{Sn}$	0.222	$^{109}\text{Mo} + ^{133}\text{Te}$	0.128
	$^{77}\text{Zn} + ^{165}\text{Gd}$	0.120	$^{116}\text{Rh} + ^{126}\text{In}$	0.087
	$^{79}\text{Ga} + ^{163}\text{Eu}$	0.095	$^{112}\text{Ru} + ^{130}\text{Sn}$	0.072
	$^{82}\text{Ge} + ^{160}\text{Sm}$	0.094	$^{77}\text{Zn} + ^{165}\text{Gd}$	0.059

we get many neutron fragment in that region [17]. Although, the even-even fragments are more possible fission yield, in the present case, we find maximum number of fission yield is odd mass fragments as compared to the even-even combination. Because of the level density of the odd mass fragments are higher than the even mass fragments as reported in Ref. [2]. For this temperature, all nuclei become spherical, the excitation energy of the closed shell nuclei is higher than the other spherical nuclei. Thus, the deformation of the fission fragments affects the most favorable distribution at the temperatures $T = 1-2$ MeV. In FRDM model the temperature dependent deformations are not considered, so the most favorable fragments at $T = 2$ and 3 MeV are same.

4. Summary and Conclusions

The binary fission mass distribution is studied within the statistical theory. The level densities and the excitation energies are calculated from the TRMF and FRDM formalisms. The TRMF model includes the thermal evolutions of the pairing gaps and deformation in a self-consistent manner, while, they are ignored in the FRDM. The excitation energies of the fragments are obtained from ground state results in the FRDM calculations. So, the study of deformation effects on the fission fragments can be seen within the TRMF formalism. The quadrupole deformations of fission fragments with the increasing temperature are also discussed. The structural effects of the fission fragments influence the most favorable yields at temperatures $T = 1$ and 2 MeV. For the temperature $T = 3$ MeV, one of the most favorable mass distribution ends up in the vicinity or exactly at the nucleon closed shell ($N \sim 82$) or (N or $Z = 50$). Although, the TRMF and FRDM formalisms yield the closed shell nucleus as one of the favorable fragment, the detail of the fission yields and probability of the mass distributions are quite different in these two formalisms.

The author MTS acknowledge that the financial support from UGC-BSR research grant award letter no. F.25-1/2014-15(BSR)7-307/2010/(BSR) dated 05/11/2015 and IOP, Bhubaneswar for the warm hospitality and for providing the necessary computer facilities.

References

- [1] P. Lichtner, D. Drechsel, J. Maruhn and W. Greiner, Phys. Lett. B **45**, 175 (1978).
- [2] P. Fong, Phys. Rev. **102**, 434 (1956).
- [3] M. Rajasekaran and V. Devanathan, Phys. Rev. C **24**, 2606 (1981).
- [4] M. Balasubramaniam, C. Karthikraj, N. Arunachalam and S. Selvaraj, Phys. Rev. C **90**, 054611 (2014).
- [5] M.T. Senthil kannan, C. Karthikraj, K. R. Vijayaraghavan and M. Balasubramaniam, (to be published).
- [6] P. Möller, J. R. Nix and K. L. Kratz, At. Data and Nucl. Data Tables **59**, 185 (1995).
- [7] B. K. Agrawal, Tapas Sil, J. N. De and S. K. Samaddar, Phys. Rev. C **62**, 044307 (2000); *ibid* **63**, 024002 (2001).
- [8] M.T. Senthil kannan, Bharat Kumar, M. Balasubramaniam, B. K. Agrawal, S. K. Patra (to be published)
- [9] D. W. Bergen and R. R. Fullwood, Nucl. Phys. A **163**, 577 (1971).

- [10] A. J. Cole, in *Fundamental and Applied Nuclear Physics Series - Statistical models for nuclear decay from evaporation to vaporization*, edited by R. R. Betts and W. Greiner, Institute of Physics Publishing, Bristol and Philadelphia, 2000.
- [11] Y. K. Gambhir, P. Ring and A. Thimet, *Ann. of Phys.* **198**, 132 (1990).
- [12] S. K. Patra and C. R. Praharaj, *Phys. Rev. C* **44**, 2552 (1991).
- [13] M. A. Preston and R. K. Bhaduri, *Structure of Nucleus*, Addison-Wesley Publishing Company, Ch. 8, page 309 (1982).
- [14] S. K. Patra, *Phys. Rev. C* **48**, 1449 (1993).
- [15] <https://www-nds.iaea.org/RIPL-3/>
- [16] A. Chaudhuri *et. al.*, *Phys. Rev. C* **91**, 044620 (2015).
- [17] L. Satpathy and S. K. Patra, *J. Phys. G: Nucl. Part. Phys.* **30**, 771 (2004).